

Advanced Applications of Optical, Microwave and Hyperspectral RS in Mongolia¹

Damdinsuren AMARSAIKHAN, Mongolia



Keywords: Optical, Microwave, Hyperspectral, Advanced applications, Analysis

Summary: The aim of this paper is to describe some advanced applications of optical, microwave and hyperspectral remote sensing (RS) in Mongolia. For this purpose, several case studies conducted for different applications are highlighted. The first case study describes the application of optical Quickbird data for urban land cover classification. The second case study describes the applications of microwave RS and it consists of three different studies. The first study highlights the polarimetric calibration of ALOS PALSAR conducted in a test site near Ulaanbaatar city, while the second study describes the urban land cover mapping using optical and synthetic aperture radar (SAR) data sets. The third study reviews the research on applications of ground penetrating radar conducted in a water source area of Ulaanbaatar city. The third case study highlights the research on applications of hyperspectral RS for urban land cover discrimination. For the final analyses, multisource satellite images with different spatial resolutions, topographic and thematic maps of varying scales as well as some ground truth data sets are used.

1. INTRODUCTION

At present, because of the rapid development of a human society and the related newly emerging issues, appropriate planning and management are becoming the major tasks of governments in both developed and developing countries. For any planning and management, the detailed and real-time spatial information can play an important role. For example, such information can be successfully used for many different disciplines including social planning, land cover/use change detection, natural resources assessment, urban planning, environmental management and many others (Amarsaikhan and Sato 2003). In general, spatial information can be collected from a number of sources such as a field survey, planning maps, topographic maps, digital cartography, thematic maps, global positioning system and RS. Of these, only

¹ In 4 different case studies the capabilities of these techniques and the usage nowadays in Mongolia are demonstrated. This paper was presented at the FIG Commission 5 and 6 workshop in September 2011 in Ulaan-Baatar. The author, Prof. Damdinsuren Amarsaikhan is Head of the Geoinformatics Laboratory at the Institute of Informatics and Remote Sensing, Mongolian Academy of Sciences and Professor at the National University of Mongolia.

RS can provide detailed real-time information that can be used for the real-time spatial analysis (Amarsaikhan *et al.* 2009b).

Over the past few years, RS platforms, techniques and technologies have been evolutionized. System capabilities have greatly improved and the costs for the primary RS data sets have been drastically decreased. Meanwhile, much satellite information can be available free of charge from different sources on the Internet. Now the highest spatial resolution images can be acquired with centimeters-accuracy, whereas the ordinary high-resolution images can be acquired with a few meters accuracy. This means that it is possible to extract different thematic information of varying scales from RS images having different spatial and spectral resolutions (Amarsaikhan *et al.* 2009a). Moreover, it is possible to integrate the extracted from RS information with other historical data sets stored in a geographical information system (GIS) and conduct sophisticated analyses (Amarsaikhan *et al.* 2011).

Traditionally, multispectral RS images have been widely used for different thematic applications. Since the end of the last century, SAR and hyperspectral data sets have been increasingly available for the RS specialists. It has been found that the images acquired at different portions of electro-magnetic spectrum provide unique information when they are integrated. For example, optical data contains information on the reflective and emissive characteristics of the Earth surface features, while the microwave data contains information on the surface roughness, texture and dielectric properties of natural and man-made objects (Amarsaikhan *et al.* 2007). Unlike the data sets from these sources, hyperspectral images provide very detailed information about the spectral behaviour of different features.

Mongolia has an extensive area (about 1.565.000sq.km) in comparison with its sparsely populated 2.8 million inhabitants. In addition, the country is very rapidly developing and there are tremendous needs for the updated spatial information. Therefore, RS can play a vital role for a thematic mapping as well as planning and management. The aim of this paper is to demonstrate some studies conducted in different test areas of Mongolia based on optical, microwave and hyperspectral RS. For this purpose, several case studies conducted for different applications have been described. For the final analyses, multisource satellite images with different spatial resolutions as well as topographic and thematic maps of varying scales have been used and different RS and GIS techniques were applied.

2. CASE STUDIES

2.1. Case study-1: Application of Optical RS for Urban Land Cover Classification

The aim of this study is to classify urban land cover types using Quickbird image. For the identification of urban land-cover types a knowledge-based classification technique based on a rule-based approach has been constructed. The constructed method uses an initial image segmentation procedure based on a Mahalanobis distance classifier as well as the constraints on spectral and spatial thresholds. The result of the knowledge-based method was compared with a result of a statistical maximum likelihood classification (MLC) and it demonstrated higher accuracy.

Test site and data sources

As a test site, Baga toiruu area situated in central part of Ulaanbaatar, the capital city of Mongolia has been selected. The Baga toiruu is the city business district of Ulaanbaatar where different government, educational, cultural and commercial organizations are located. The

location of the Baga toiruu area represented in a panchromatic Quickbird image of 2006 is shown in figure 1a.

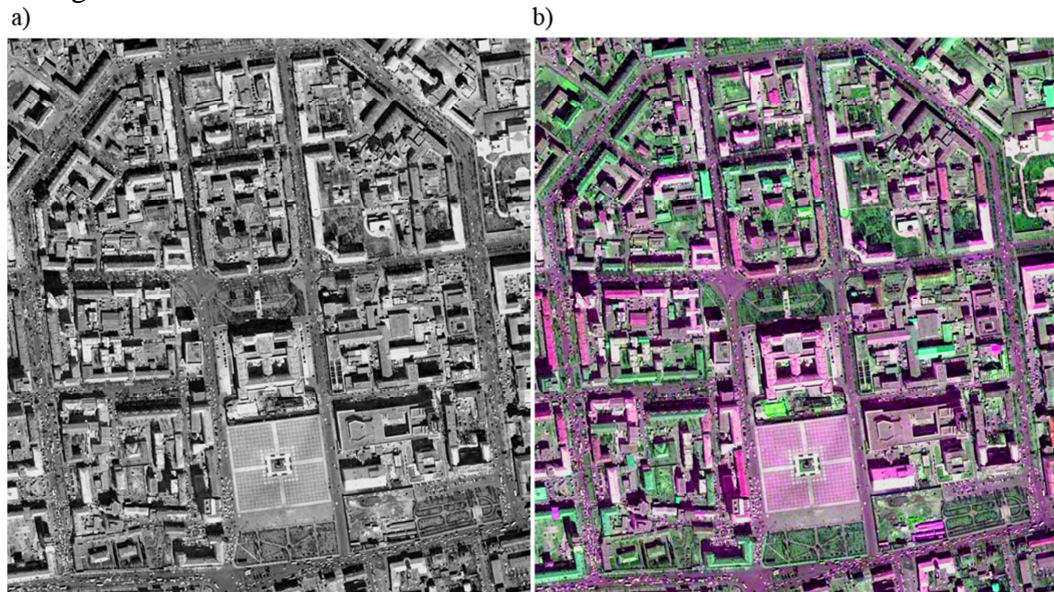


Figure 1. The test area represented in a panchromatic Quickbird image of 2006 (a), the Brovey transformed image of the test area (b).

As the RS data sources, multispectral and panchromatic Quickbird images of 2006 have been used. The Quickbird data has four multispectral bands (B1: 0.45–0.52 μm , B2: 0.52–0.60 μm , B3: 0.63–0.69 μm , B4: 0.76–0.90 μm) and one panchromatic band (Pan: 0.45-0.9 μm). The spatial resolution is 0.63m for the panchromatic image, while it is 2.44m for the multispectral bands. The high spatial resolution of the panchromatic image can distinguish most small elements at an object level which multispectral bands cannot fully resolve. Therefore, a combination of panchromatic and multispectral bands gives a real colour view of a scene. In the current study, in addition to the Quickbird images, a topographic map of 2000, scale 1:5000 and a GIS layer created on the basis of the topographic map, were available.

Knowledge-based classification

Over the past years, knowledge-based techniques have been widely used for the classification of RS images. The knowledge in image classification can be represented in different forms depending on the type of knowledge and necessity of its usage (Amarsaikhan and Douglas 2004). The most commonly used techniques for knowledge representation are a rule-based approach and neural network classification (Amarsaikhan *et al.* 2007). In the present study, for discrimination of the urban land-cover types a rule-based approach has been applied.

As we had data sets with different spatial and spectral resolutions, they should be merged for conducting further analyses. In this study, to merge the images, Brovey transform and principal component analysis (PCA) (Gonzalez *et al.* 2004) have been applied and the results were compared. For the Brovey transform, the bands of 2,3 and 4 were considered as the multispectral bands, while the panchromatic Quickbird image was considered as the higher spatial resolution band. The PCA has been performed using the available panchromatic and multispectral bands. As it was seen from the PCA, the first three PCs contained almost 98.6% of the total variance. The inspection of the last PC indicated that it contained noise from the total dataset. Therefore, it was excluded from the analysis.

In order to obtain a reliable image that can illustrate the spectral and spatial variations in the selected classes of objects, different band combinations have been compared. Although, the image created by the Brovey transform contained some shadows that were present on the panchromatic image, it still illustrated good result in terms of separation of the available land use classes and individual objects. The image created by the PCA method contained less shadows, however, it was very difficult to analyze the final image, because it contained too much color variation of objects belonging to the same class. Therefore, for further analysis the image created by the Brovey transform has been used. As seen from the Brovey transformed image shown in figure 1b, all details are clearly seen.

To extract the urban land cover information, a rule-based approach which consists of a set of rules, that contains the initial image segmentation procedure based on a Mahalanobis distance classifier (Mather 1999) and the constraints on spectral parameters and spatial thresholds, has been constructed. In the Mahalanobis distance estimation, for the initial separation of the classes, only pixels falling within 1.0-1.5 standard deviation (SD) and the Brovey transformed features were used. The pixels falling outside of 1.0-1.5 SD were temporarily identified as unknown classes and further classified using the rules in which different spectral and spatial thresholds were used. The spectral thresholds were determined based on the knowledge about spectral characteristics of the selected classes, whereas the spatial thresholds were determined based on polygon boundaries of the created GIS layer. The image classified by this method is shown in figure 2b. As seen from the classified image, the rule-based approach could very well separate all individual objects. For the accuracy assessment of the classification result, the overall performance has been used. As ground truth information, for each class several regions containing the total of 3268 purest pixels have been selected. The confusion matrix indicated an overall accuracy of 98.26%.

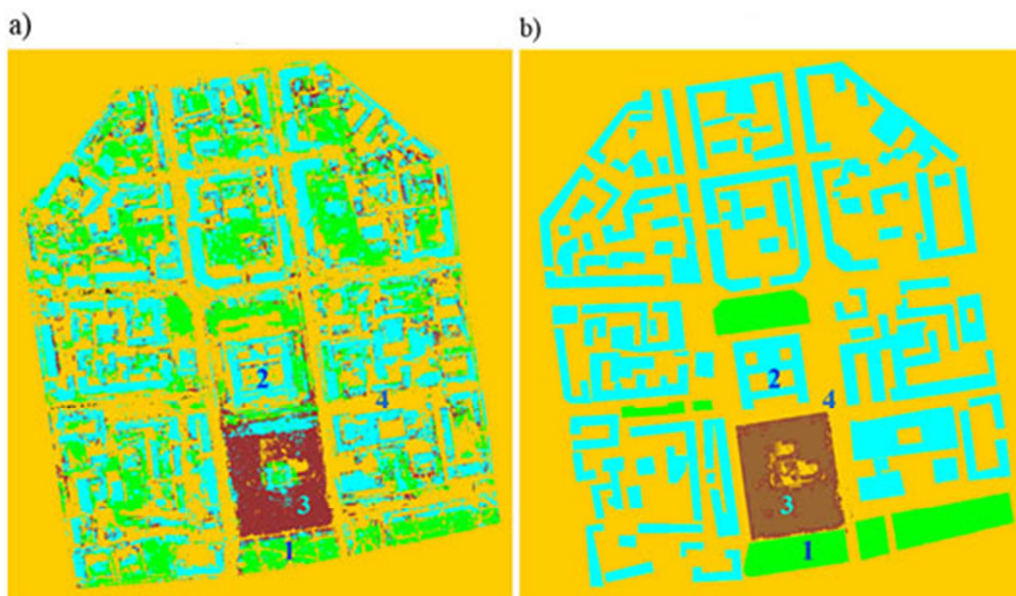


Figure 2. a) The result of the MLC, b) The result of the rule-based method.
(1-Vegetation, 2-Builtup area, 3-Central square, 4-Open area).

To compare the performance of the developed algorithm and a standard method, the same set of features and training signatures used for the rule-based classification, were classified using

the statistical MLC. The image classified by the MLC method is shown in figure 2a. The confusion matrix indicated an overall accuracy of 86.34%. As seen from the classification results shown in figure 2, the result of the rule-based method looks much better than that of the standard method and the extracted objects are very accurately delineated forming the classes of objects.

2.2. Case study-2: Applications of Microwave RS

Case study-2a: Polarimetric Calibration of ALOS PALSAR Data

The aim of this study is to carry out polarimetric calibration of ALOS PALSAR data. PALSAR operates in L-band (1.27GHz) and is capable to observe the ground surface conditions accurately compared to other SAR systems operating at higher frequencies, namely C-band or X-band. The data acquisition for polarimetric calibration was conducted on 25 May 2006. Corner reflectors were set in a flat area inside the Chingis Khan International airport. The ground surface was covered by grass, having about 30cm height. In the study, 4 corner reflectors were set and they were aligned along a straight line parallel to the run way, and each corner reflector was separated by 100m from each other (Sato *et al.* 2010).

Figure 3 shows the polarimetric SAR images (the single bounce (a), the double bounce (b) and the volume scattering (c) components) represented using a Pauli decomposition. We can find the locations of 3 dihedral corner reflectors in Figure 3a and they represent the single bounce component of the polarimetric SAR image. The dihedral corner reflector can be seen in Figure 3b and it represents the double-bounce component of the polarimetric SAR image. As could be seen that the background scattering is stronger than the expected one and it is probably due to the shallow off-nadir angle 21.5° which was used during the data acquisition.

As we could determine the locations of the corner reflectors from the polarimetric SAR images, it is possible to pick up the polarimetric scattering coefficients from the SAR images in order to confirm the polarimetric characteristics of the SAR images. After calculating, scattering matrices for the trihedral and dihedral corner reflectors, it was possible to confirm that for all corner reflectors, the measured scattering matrices well corresponded to the theoretical ones. Figure 4 shows the polarimetric PALSAR image of Ulaanbaatar area acquired in May 2006. As seen from the image, the city and bare ground are dominated by the HH and VV components, while the mountain area is dominated by HV component (Sato *et al.* 2010).

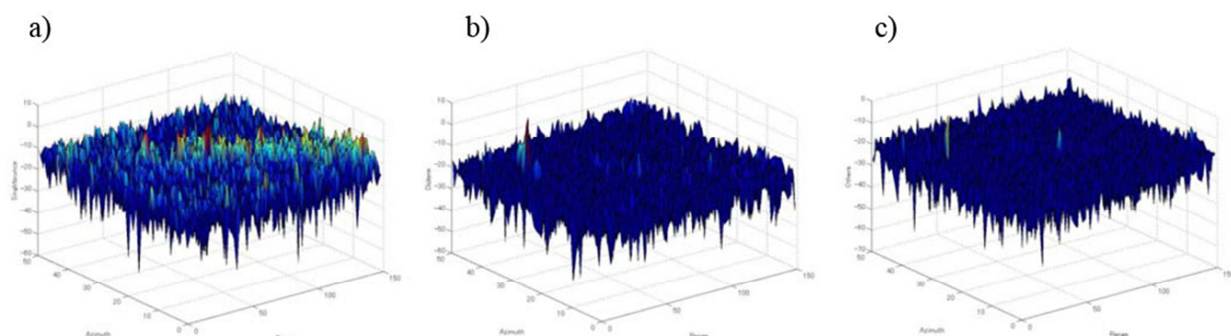


Figure 3. The polarimetric SAR images represented using a Pauli decomposition. (a) the single bounce, (b) the double bounce and (c) the volume scattering components.



Figure 4. Polarimetric PALSAR image of Ulaanbaatar area.

Case study-2b: Urban Land Cover Mapping using Optical and SAR Data sets

In recent years, very high spatial resolution optical and SAR data sets have become increasingly available from space platforms and this makes it possible to extract very detailed land cover information from such data. Over the past decade, the integrated features of the optical and microwave data sets have been efficiently used for an improved land cover mapping. Many authors have proposed different techniques to separate the existing land cover classes from the combined optical and SAR images and they all judged that the results were better. The main aim of this study is to evaluate the features from the combined optical and microwave data sets in terms of separation of urban land cover types. For this purpose, a refined Bayesian classification algorithm has been constructed. For the actual analysis, very high resolution TerraSAR and Quickbird images of Ulaanbaatar area, Mongolia were used.

Co-registration of the images and speckle suppression of the TerraSAR

In order to perform accurate data fusion, both high geometric accuracy and good geometric correlation between the images are needed. As a first step, the Quickbird image was georeferenced to a Gauss-Kruger map projection using 9 ground control points (GCPs) defined from a field survey. The GCPs have been selected on clearly delineated crossings of roads, streets and city building corners. For the transformation, a second-order transformation and nearest-neighbour resampling approach were applied and the related root mean square error (RMSE) was 1.06 pixel. Then, the TerraSAR image was geometrically corrected and its coordinates were transformed to the coordinates of the georeferenced Quickbird image. In order to correct the SAR image, 15 more regularly distributed GCPs were selected from different parts of the image. For the actual transformation, a second-order transformation was used. As a resampling technique, the nearest-neighbour resampling approach was applied and the related RMSE was 1.48 pixel. As both optical and microwave images had a very high

spatial resolution, the errors of less than 1.5m were considered as acceptable for further studies (Amarsaikhan *et al.* 2010).

As microwave images have a granular appearance due to the speckle formed as a result of the coherent radiation used for radar systems; the reduction of the speckle is a very important step in further analysis. The analysis of the radar images must be based on the techniques that remove the speckle effects while considering the intrinsic texture of the image frame (Serkan *et al.* 2008). In this study, five different speckle suppression techniques such as local region, median, lee-sigma, frost and gammamap filters (Amarsaikhan and Saandar 2011) of 5x5 and 7x7 sizes were compared in terms of delineation of urban features and texture information. After visual inspection of each image, it was found that the 5x5 gammamap filter created the best image in terms of delineation of different features as well as preserving content of texture information. In the output image, speckle noise was reduced with very low degradation of the textural information.

Derivation of features and standard Bayesian classification

Initially, in order to increase the spatial homogeneity of the data, to the TerraSAR image, a 3x3 average filtering was applied. Then, to derive texture features from the multisource images, contrast, entropy and dissimilarity measures (using a 15x15 window size) have been applied and the results were compared. The bases for these measures are the co-occurrence measures that use a grey-tone spatial dependence matrix to calculate texture values, and the matrix shows the number of occurrences of the relationship between a pixel and its specified neighbor (ENVI 1999). The contrast measure indicates how most elements do not lie on the main diagonal, whereas, the entropy measures the randomness and it will have its maximum when all elements of the co-occurrence matrix are the same. The dissimilarity measure indicates how different the elements of the co-occurrence matrix are from each other (Karathanassi *et al.* 2007). By applying these measures, initially 15 features have been derived, but after thorough checking of each individual feature only 4 features, including the results of the entropy measure applied to HH polarization image of TerreaSAR and infrared band of Quickbird, and the results of the dissimilarity measure applied to VV polarization image of TerreaSAR and infrared band of Quickbird, were selected.

To define the sites for the training signature selection from the multisensor images, two to four areas of interest (AOI) representing the available six classes (built-up area, ger area, open area, road, central square and ice) have been selected through analysis of the fused images. As the data sources included both optical and SAR features, the fused images were very useful for the determination of the homogeneous AOI as well as for the initial intelligent guess of the training sites. The separability of the training signatures was firstly checked in feature space and then evaluated using Jeffries–Matusita distance. After the investigation, the samples that demonstrated the greatest separability were chosen to form the final signatures. The final signatures included about 3415–10534 pixels. For the classification, the following feature combinations were used:

1. The original spectral bands of the Quickbird data.
2. The HH and VV polarization components of TerreaSAR and original spectral bands of the Quickbird data.
3. Multiple bands including the original TerreaSAR and Quickbird images as well as four other derivative bands obtained from texture measures.

4. The PC1, PC2, PC3 and PC4 of the PCA (PCA was performed using 9 bands including the original TerraSAR and Quickbird images as well as four texture features and, the first four PCs included 99.9% of the overall variance).

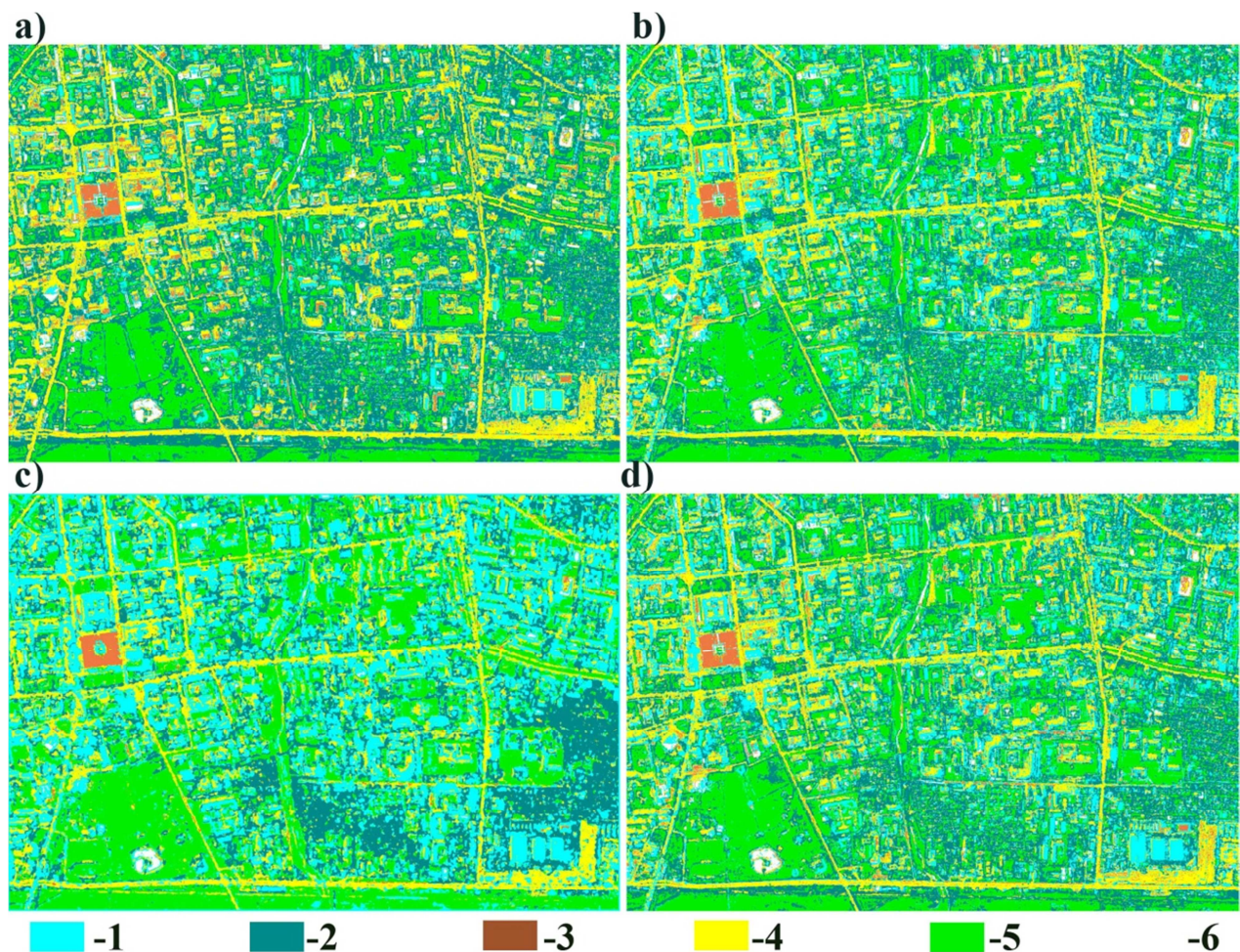


Figure 5. Comparison of the supervised classification results for the selected classes (1-built-up area; 2-ger area; 3-central square; 4-roads; 5-open area; 6-snow-ice). Classified images (a) using Quickbird bands, (b) using Quickbird and TerraSAR bands, (c) using multiple bands, (d) using the PCs.

For the actual classification, standard Bayesian MLC has been used assuming that the training samples have the Gaussian distribution (Richards and Jia 1999). To increase the reliability of the classification, to the initially classified images, a fuzzy convolution with a 5x5 size window was applied. The fuzzy convolution creates a thematic layer by calculating the total weighted inverse distance of all the classes in a determined window of pixels and assigning the centre pixel the class with the largest total inverse distance summed over the entire set of fuzzy classification layers, i.e. classes with a very small distance value will remain unchanged while the classes with higher distance values might change to a neighboring value if there are a sufficient number of neighboring pixels with class values and small corresponding distance values (ERDAS 1999). The visual inspection of the fuzzy convolved images indicated that there are some improvements on the borders of the neighboring classes that significantly influence the separation of the decision boundaries in multidimensional feature space. The

final classified images are shown in figure 5(a–d). As seen from figure 5(a–d), the classification result of the Quickbird image gives the worst result, because there are high overlaps among classes: built-up area, ger area and open area. However, these overlaps decrease on other images for the classification of which SAR and optical bands as well as other derivative features have been used. As could be seen from the overall classification results, although the combined use of optical and microwave data sets produced a better result than the single source image, it is still very difficult to obtain a reliable land cover map by the use of the standard technique, specifically on decision boundaries of the statistically overlapping classes (Amarsaikhan *et al.* 2010).

For the accuracy assessment of the classification results, the overall performance has been used. As ground truth information, different AOIs containing 56,864 purest pixels have been selected. AOIs were selected on a principle that more pixels to be selected for the evaluation of the larger classes such as built-up area and open area than the smaller classes such as central square and snow-ice. The overall classification accuracies for the selected classes were 69.24%, 75.37%, 81.96% and 76.92% for the original spectral bands of Quickbird, TerraSAR and Quickbird data, multiple bands, and PC1, PC2, PC3 and PC4, respectively.

The refined Bayesian classification

Unlike the traditional Bayesian classification, the constructed classification algorithm uses spatial thresholds defined from the local knowledge. The local knowledge was defined on the basis of the spectral variations of the land surface features on the fused images as well as the texture information delineated on the dissimilarity images. It is clear that a spectral classifier will be ineffective if applied to the statistically overlapping classes such as built-up area and ger area because they have very similar spectral characteristics. For such spectrally mixed classes, classification accuracies should be improved if the spatial properties of the classes of objects could be incorporated into the classification criteria. The idea of the spatial threshold is that it uses a polygon boundary to separate the overlapping classes and only the pixels falling within the threshold boundary are used for the classification. In that case, the likelihood of the pixels to be correctly classified will significantly increase, because the pixels belonging to the class that overlaps with the class to be classified using the threshold boundary are temporarily excluded from the decision making process. In such a way, the image can be classified several times using different threshold boundaries and the results can be merged (Amarsaikhan and Sato 2004).

The result of the classification using the refined method is shown in figure 6. For the accuracy assessment of the classification result, the overall performance has been used, taking the same number of sample points as in the previous classifications. The confusion matrix produced for the refined classification method showed overall accuracy of 90.96%. As could be seen from figure 6, the result of the classification using the refined Bayesian classification is much better than result of the standard method.



Figure 6. Classification result obtained by the refined method.

Case study-2c: Application of Ground Penetrating Radar

Ground penetrating radar (GPR) is known as a very powerful geophysical exploration technique for subsurface sensing. The aim of this study is to assess the potential of a GPR for detecting and monitoring groundwater movement and estimate the hydraulic properties of an aquifer. For this purpose, GPR surveys have been conducted at a water source area of Ulaanbaatar city.

In general, Ulaanbaatar city solely depends on the groundwater withdrawn from an alluvial aquifer, distributed in the Tuul River basin, which is mainly located in the southern part of the city. The water is supplied from water production wells. At present, with the increase in population and rapid economic development, Ulaanbaatar city is facing water shortages. Therefore, assessing the groundwater from a well and its production capacity has become very important for all citizens of the capital city. If the groundwater level change around the production well can be observed by GPR, it will provide much useful information about the aquifers. The groundwater level in the Ulaanbaatar city area is between 2-10 m, and the GPR technique is suitable for detecting this relatively shallow aquifer (Sato *et al.* 2010).

Within the framework of the present study, field experiments were conducted in Ulaanbaatar in October 2001 and in April 2002. The GPR survey lines were located around a pumping well. By varying the water production, GPR was used for detecting the change of groundwater conditions around the well. An appropriate approach for estimating hydraulic properties involves the development of a detailed model of the aquifer system. This study focuses on the practical use of GPR for groundwater monitoring, tries to quantify the groundwater level change, and estimates the hydraulic properties by assuming a model of the aquifer system.

Figure 7 shows the GPR profiles measured at a low water condition as well as a high water condition, which were controlled by a pumping operation. As seen from the figure 7, one can very clearly observe the change of the ground water condition.

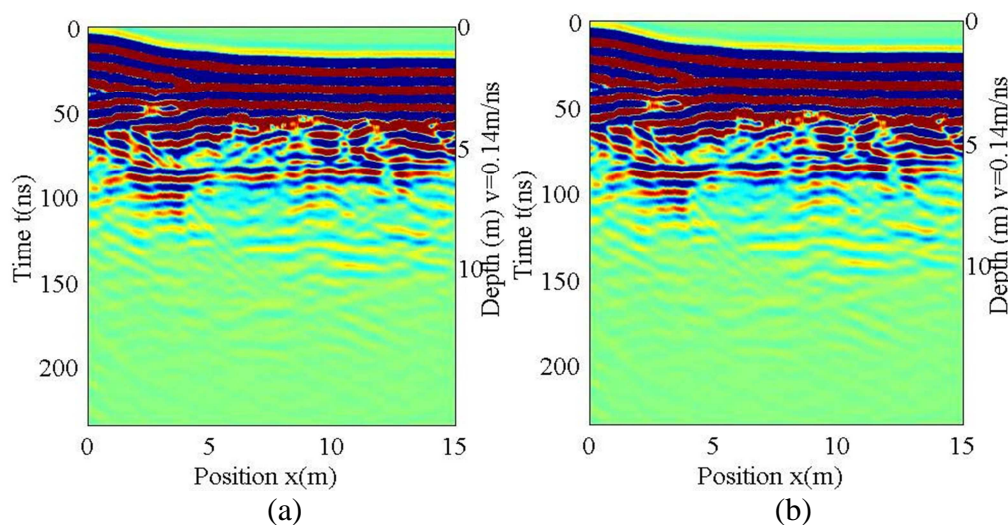


Figure 7. GPR profiles acquired along survey line N on 4 and 5 October 2001.
 (a) During pumping (water level in the well was 6.45 m).
 (b) After recovery (water level in the well was 5.8 m).

2.3. Case study-3: Application of Hyperspectral RS

In recent years, processing of hyperspectral data has attracted many researchers dealing with RS image processing. Unlike the traditional multispectral data taken in the optical range of electro-magnetic spectrum, the hyperspectral data deals with a great number of bands and many attempts are being made to reduce the dimensionality of the data and extract reliable information needed for various decision-making processes. Especially, for classification applications, hyperspectral data sets provide enormous potential for an improved discrimination between the land cover types or features having very similar spectral characteristics (Amarsaikhan and Ganzorig 1999, Demir and Erturk 2008). The aim of this study is to classify urban land cover types using Hyperion hyperspectral data sets.

Hyperion is a hyperspectral sensor launched by NASA in November 2000 and it marked the establishment of spaceborne hyperspectral mapping capabilities. It covers $0.4\mu\text{m}$ to $2.5\mu\text{m}$ spectral range with 242 spectral bands at approximately 10nm spectral resolution and the data has 30m spatial resolution. The instrument captures 256 spectra over a 7.5km-wide swath perpendicular to the satellite motion (Kruse 2002). In the present study, a Hyperion image of Ulaanbaatar area taken on 18 August 2002 has been used. For the land cover classification, a spectral angle mapper method was used. The spectral angle mapper is one of the most widely used hyperspectral classification techniques and it uses an n -dimensional angle to match pixels to reference spectra. The method determines the spectral similarity between two spectra by calculating the angle between the spectra, treating them as vectors in a space with dimensionality equal to the number of bands.

To evaluate the performance of the hyperspectral data for a land cover discrimination, the result of the Hyperion image classification was compared with a result of Landsat ETM image of August 2002. Figure 8(a-d) shows the original Hyperion and Landsat ETM images and their classified results. As seen from the figure 8, although both images performed well, still hyperspectral image performed better in terms of discrimination between fuzzy classes: green vegetation (grass) and deciduous forest as well as between deciduous forest and coniferous forest. The advantage of a hyperspectral image is that looking at a spectral curve, one can select the most separable bands and use them for the improved classification. The comparison of the spectral curves of the selected classes (ie, urban area, soil, green vegetation, deciduous forest, coniferous forest and water) is shown in figure 9. As seen from the figure, the hyperspectral image has much more advantage than the ordinary multispectral image.

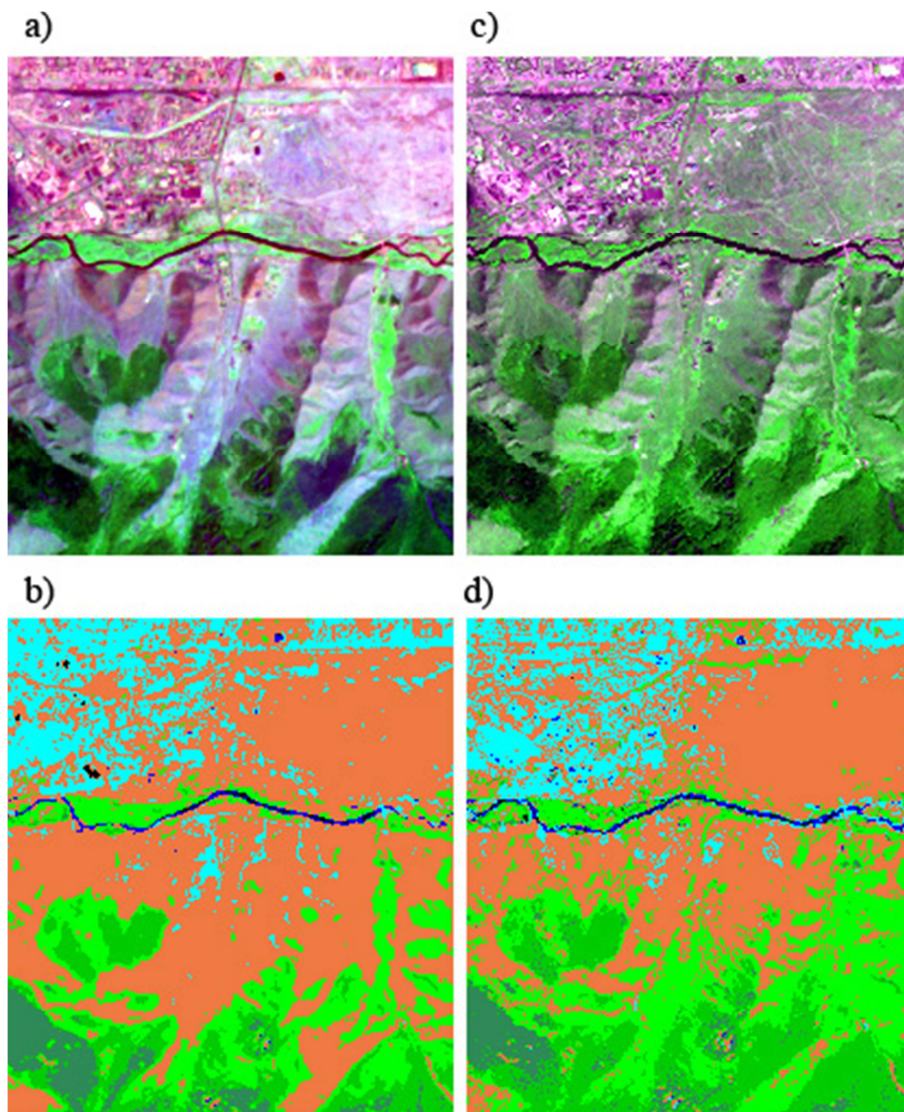


Figure 8. The original Hyperion (a) and Landsat ETM (c) images.
The classified images of Hyperion (b) and Landsat ETM (d).

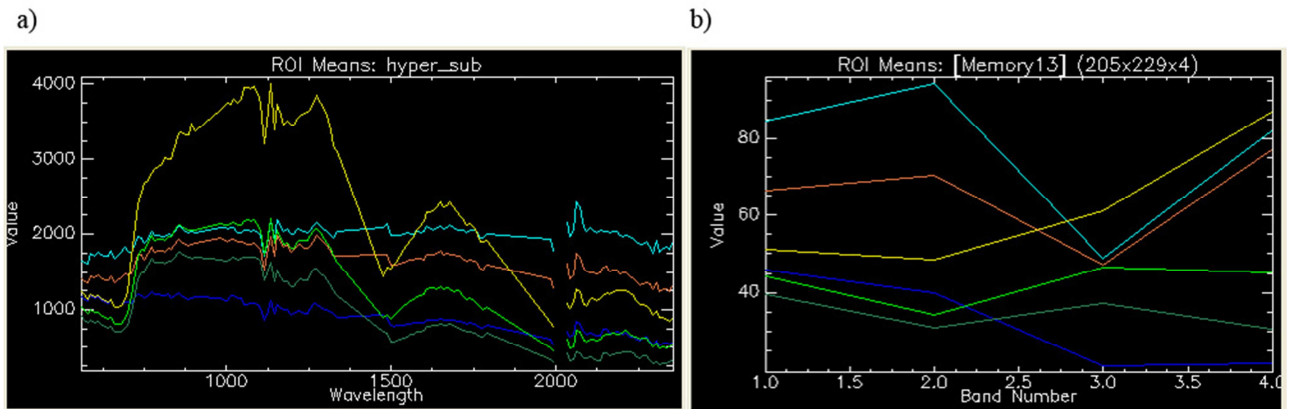


Figure 9. Spectral curves of the selected classes in Hyperion (a) and Landsat ETM (b) images.

Moreover, it is possible to check the reliability of the selected features on a feature space and validate them for further classification analysis. Figure 10 shows the highly correlated and less correlated features. As seen from the figure 10, neighboring bands have very high correlation, while the bands selected from different ranges have less correlation.

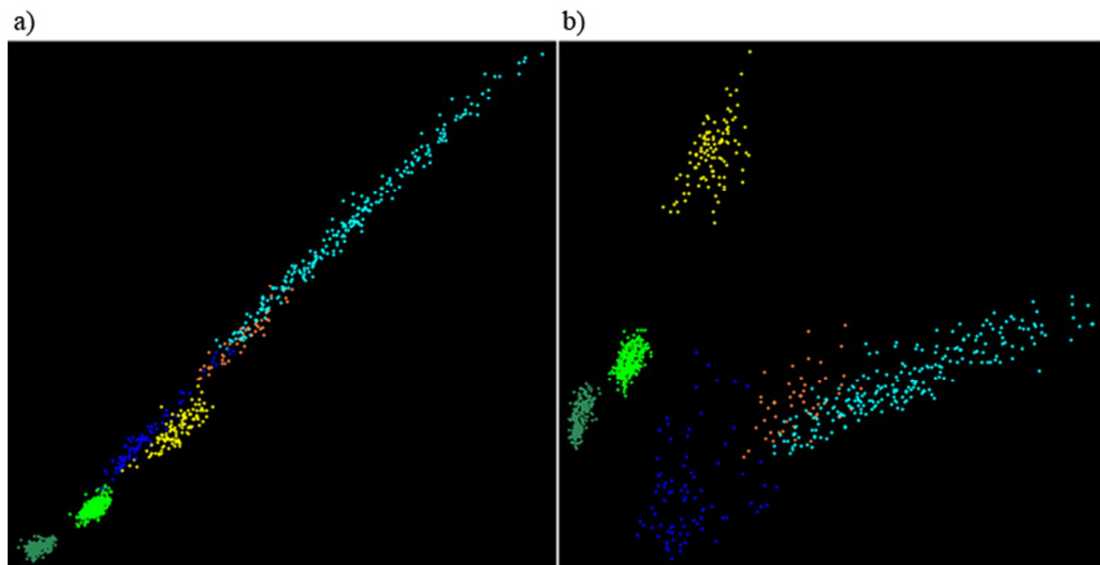


Figure 10. The highly correlated (a) and less correlated (b) bands.

3. CONCLUSIONS

The aim of this research was to apply some advanced techniques based on optical, microwave and hyperspectral RS for different thematic studies in Mongolia. For this purpose, several case studies were highlighted. The first case study described the combined use of panchromatic and multispectral

Quickbird images of Ulaanbaatar city for urban land cover classification. The second case study highlighted three different applications of microwave RS. The first application described the polarimetric calibration of ALOS PALSAR conducted in a test site near Ulaanbaatar city and further backscatter analysis of polarimetric characteristics. The second application highlighted an integrated use of multispectral Quickbird and polarimetric TerraSAR images

for an improved urban land cover mapping. The third application reviewed the research on the use of GPR technology for determination of a ground water level in a water source area of Ulaanbaatar city. The third case study described the applications of hyperspectral RS for an urban land cover mapping where the classification result of a 242 band Hyperion image was compared with the result of Landsat ETM image. Overall, the study demonstrated that the multisource RS data sets could significantly improve land cover analyses, and support planning and management.

REFERENCES

Amarsaikhan, D. and Ganzorig, M., 1999, Different approaches in feature extraction for hyperspectral image classification, Invited paper published in Proceedings of the 20th Asian Conference on RS, Hong Kong, pp.434-438.

Amarsaikhan, D. and Sato, M., 2003, The role of high resolution satellite images for urban area mapping in Mongolia, Full paper published in the 'Reviewed Papers' part of Proceedings of the Computers for Urban Planning and Urban Management (CUPUM)'03 International Conference, Sendai, Japan, pp.1-12.

Amarsaikhan, D. and Douglas, T., 2004, Data fusion and multisource data classification, International Journal of Remote Sensing, No.17, Vol.25, pp.3529-3539.

Amarsaikhan, D. and Sato, M., 2004, Validation of the Pi-SAR data for land cover mapping, Journal of the Remote Sensing Society of Japan, No.2, Vol.24, pp.133-139.

Amarsaikhan, D., Ganzorig, M., Ache, P. and Blotevogel, H., 2007, The integrated use of optical and InSAR data for urban land cover mapping, International Journal of Remote Sensing, Vol.28, No.6, pp.1161-1171.

Amarsaikhan, D., Blotevogel, H.H., Ganzorig, M. and Moon, T.H, 2009a, Applications of remote sensing and geographic information systems for urban land-cover changes studies in Mongolia, Geocarto-International, A Multi-Disciplinary Journal of Remote Sensing and GIS, Vol. 24, No. 4, August 2009, 257–271.

Amarsaikhan, D., Ganzorig, M., Blotevogel, H.H., Nergui, B. and Gantuya, R., 2009b, Integrated method to extract information from high and very high resolution RS images for urban planning, Journal of Geography and Regional Planning, Vol. 2(10), pp. 258-267.

Amarsaikhan, D., Blotevogel, H.H., van Genderen, J.L., Ganzorig, M., Gantuya, R. and Nergui, B., 2010, Fusing high resolution TerraSAR and Quickbird images for urban land cover study in Mongolia, International Journal of Image and Data Fusion, Vol.1, No.1, pp.83-97.

Amarsaikhan, D. and Saandar, M., 2011, Chapter - "Fusion of Multisource Images for Update of Urban GIS" in "IMAGE FUSION" BOOK published by InTECH Open Access Publisher, pp.1-26.

Amarsaikhan, D., Chinbat, B. and Ganzorig, M., 2011, Applications of RS and GIS for urban land use change study in Ulaanbaatar city, Mongolia, Journal of Geography and Regional Planning Vol. 4(8), pp. 471-481.

Demir, B. and Erturk.S., 2008, Improved classification and segmentation of hyperspectral images using spectral warping, *IJRS*, Vol.29, 12, 3657-3663.

ENVI, 1999, User's Guide, Research Systems.

ERDAS, 1999, Field guide, Fifth Edition, ERDAS, Inc. Atlanta, Georgia.

Gonzalez, A.M. Saleta, J.L. Catalan, R.G. Garcia, R., 2004, Fusion of multispectral and panchromatic images using improved IHS and PCA mergers based on wavelet decomposition. *IEEE Transactions Geoscience and Remote Sensing*, 6, pp.1291- 1299.

Karathanassi, V., Kolokousis, P. and Ioannidou, S., 2007, A comparison study on fusion methods using evaluation indicators, *International Journal of Remote Sensing*, 28, pp.2309 – 2341.

Kruse, F.A., 2002, Comparison of AVIRIS and Hyperion for hyperspectral mineral mapping, 11th JPL Airborne Geoscience Workshop, 4-8 March 2002, Pasadena, California.

Mather, P.M., 1999, *Computer Processing of Remotely-Sensed Images: An Introduction*, Second Edition, (Wiley, John & Sons).

Richards, J. A. and Jia, S., 1999, *Remote Sensing Digital Image Analysis—An Introduction*, 3rd edn (Berlin: Springer-Verlag).

Sato, M., Tseedulum, K. and Amarsaikhan, D., 2010, GPR and Polarimetric SAR Observation of Environment of Mongolia, Full paper published in Proceedings of the XVII International Symposium of Kherlen Geological Expedition, Ulaanbaatar, Mongolia.

Serkan, M., Musaoglu, N., Kirkici, H. and Ormeci, C., 2008, Edge and fine detail preservation in SAR images through speckle reduction with an adaptive mean filter, *International Journal of Remote Sensing*, Volume 29, Issue 23, First published 2008, pp.6727 – 6738.

BIOGRAPHY OF ACADEMICIAN DAMDINSUREN AMARSAIKHAN

Academician Damdinsuren Amarsaikhan, Head of Geoinformatics Laboratory, Institute of Informatics and RS, Mongolian Academy of Sciences and Professor at National University of Mongolia was born in 1964 in Mongolia.

In 1997 he obtained a PhD Degree from the Mongolian Technical University. His thesis entitled “Update of a GIS by RS data using a knowledge-based approach” describes the part of his research on design and implementation of a spatial decision support system, and its update by RS data. In 2006, he defended a Degree of Doctor of Science at the Mongolian Academy of Sciences. His thesis entitled “Scientific basis for update of integrated GIS by multisource information” describes a systematic approach to update an integrated GIS by the information from different sources.

He was a visiting professor and researcher at the German Aerospace Research Establishment-DLR (1997), University of Newcastle, UK (2001), University of Dortmund (2005) and Geyongsang National University, Korea (2005, 2006, 2007 and 2008). From August 2002 to

August 2004, he was a JSPS (Japan Society for the Promotion of Science) postdoctoral research fellow with research status as professor at the Center for Northeast Asian Studies, Tohoku University, Japan. In 2008-2009, he was a visiting professor of Humboldt Foundation at the Dortmund University of Technology, Germany.

His professional interests include design and implementation of GISs; development of techniques for multisource data analysis; spatial data management; urban planning and management using RS and GIS; environmental monitoring and natural resources management using RS, GIS and spatial statistics; land use/cover change study using geoinformatics methods.

He is an author and co-author of about 150 international and national papers published in the scientific journals and conference proceedings and also the main author and editor-in-chief of the books 'Principles of Remote Sensing and Geographical Information Systems' and 'Principles of Geographical Information Systems for Natural Resources Management' the books ever to be written in the Mongolian language on the subject of RS and GIS.

Academician D.Amarsaikhan is the winner of "The Young Scientist" Prize, awarded by Third World Academy of Sciences; The Advanced Scientist of Mongolia-2001; the winner of Second Prize of "The Outstanding Scientist of Mongolia-2005" Prize, the award of the Year of Mongolian Academy of Sciences and Ministry of Science and Education of Mongolia, the winner of "The Best ITC Alumni Paper Award" awarded from the ISPRS TC7 Mid-Term Symposium of 2006, the winner of Special Prize of "The Outstanding Scientist of Mongolia-2008" Prize, the winner of "The Most Outstanding IT Researcher of Mongolia-2009" Prize.

CONTACT DETAILS:

Institute of Informatics and RS, Mongolian Academy of Sciences,
av.Enkhtaivan-54B, Ulaanbaatar-51, Mongolia
Tel: 976-11-453660 Fax: 976-11-458090
E-mail: amarsaikhan64@gmail.com